Anal Bioanal Chem (2006) 384: 1320–1330
DOI 10.1007/s00216-005-0293-1

ORIGINAL PAPER

Martin Ferm · John Watt · Samantha O'Hanlon · Franco De Santis · Costas Varotsos

Deposition measurement of particulate matter in connection with corrosion studies

Received: 13 October 2005 / Revised: 9 December 2005 / Accepted: 21 December 2005 / Published online: 2 March 2006

Abstract A new passive particle collector (inert surrogate surface) that collects particles from all directions has been developed. It was used to measure particle deposition at 35 test sites as part of a project that examined corrosion of materials in order that variation in particulate material could be used in development of dose–response functions in a modern multi-pollutant environment. The project, MULTI-ASSESS, was funded by the EU to examine the effects of air pollution on cultural heritage. Passive samplers were mounted rain-protected, and both in wind-protected and wind-exposed positions, to match the exposure of the samples for corrosion studies. The particle mass and its chemical content (nitrate, ammonium, sulfate, calcium, sodium, chloride, magnesium and potassium) were analysed. The loss of light reflectance on the surrogate surface was also measured. Very little ammonium and potassium was found, and one or more anions are missing in the ion balance. There were many strong correlations between the analysed species. The mass of analysed water-soluble ions was fairly constant at 24% of the total mass. The particle mass deposited to the samplers in the wind-protected position was about 25% of the particles deposited to an openly exposed sampler. The Cl^-/Na^+ ratios indicate a reaction between HNO_3 and NaCl. The deposited nitrate flux corresponds to the missing chloride. The Ca^{2+} deposition equals the SO_4^{2-} deposition and the anion deficiency. The SO_4^{2-} deposition most likely originates from SO_2 that has reacted with basic calcium-containing particles either before or after they were deposited. The particle depositions at the urban sites were much higher than in nearby rural sites. The deposited mass correlated surprisingly well with the PM_{10} concentration, except at sites very close to traffic.

M. Ferm (✉)
IVL Swedish Environmental Research Institute,
PO Box 5302, 400 14 Gothenburg, Sweden
e-mail: Martin.Ferm@ivl.se
Tel.: +46-317-256224
Fax: +46-317-256290

J. Watt · S. O'Hanlon
School of Health and Social Sciences,
Middlesex University,
Queensway, Enfield EN3 4SA, UK

F. De Santis
CNR - Istituto Inquinamento Atmosferico,
Via Salaria Km 29,3 CP 10,
00016 Monterotondo Scalo,
Rome, Italy

C. Varotsos
Department of Applied Physics,
Laboratory of Meteorology, Panepistmioupolis,
University of Athens,
Build. Phys-5,
15784 Athens, Zografou, Greece

C. Varotsos
University of Maryland,
3419 Computer & Space Sciences Building,
College Park, MD 20742, USA

Keywords Corrosion · Cultural heritage · Sodium chloride · Passive sampler · Surrogate surface · Soiling · Calcium

Introduction

The impact of air pollution on cultural heritage has been extensively studied over a number of years, focused largely on the effects of sulfur pollutants and especially sulfur dioxide, which was identified as the most important factor for deterioration of a number of materials. During the 1990s, synergistic corrosive effects of sulfur dioxide with nitrogen dioxide and also ozone were demonstrated [1, 2].

Existing dose–response and damage functions reflect a pollution situation dominated by sulfur dioxide emissions. Recently, however, concerted international policy actions have reduced pollution from this source to a low level, in some areas close to background levels. This decreasing sulfur dioxide level in most parts of Europe has been coupled with an increase in car traffic, which has led to elevated levels of nitrogen compounds, ozone and particulates and created a new multi-pollutant situation.

This has been acknowledged inter alia in the activities within the UN ECE Convention on long-range transboundary air pollution (CLRTAP), where a multi-pollut ant, multi-effect protocol has recently been adopted. This changed pollution situation must be taken into account in the development of an improved model for the effects of pollutants on the deterioration of important material groups.

It is in this context that it has become desirable to study parameters such as the corrosive and soiling effects of particulate matter and the effect of nitric acid. Both parameters are of special interest in urban areas with dense traffic, and nitric acid is of special interest in warmer regions such as in the Mediterranean countries. These effects have been studied in an EU project named MULTI-ASSESS (http://www.corr-institute.se/MULTI-ASSESS). One primary objective of this project was to develop multi-pollutant deterioration and soiling models of wet and dry deposition of gases and particulates on materials used in objects of European cultural heritage, and to obtain dose–response functions quantifying the effects as a function of pollution and meteorological parameters. Since these parameters need to be measured by practical and low-cost methods, an initial objective was to adapt and validate passive samplers for measuring atmospheric concentrations of nitric acid and particles and to use them in a new field-sampling programme based on an existing monitoring network for materials research. If successful, this sampler will be included in a toolkit for future research at heritage sites being validated in another part of the project.

A surrogate surface exposed in the vicinity of the object of interest receives a similar net particle deposition as for example an object of cultural heritage. A surrogate surface, which is simpler to analyse than a precious object, exposed close to the object offers a better solution than a conventional particle sampler does. A surrogate surface receives the particles passively and can be used for long-term integrative sampling. Passive sampling using small samplers is ideal for sampling around objects of cultural heritage because the sampling is silent, does not need electricity and can be performed inconspicuously and with discretion. Other advantages are that technical personnel are not needed to use the samplers and that they do not need field calibration.

Use of passive samplers in this way is also desirable because it replicates the complexity of particle deposition to actual objects, which depends on many parameters such as particle concentration, its size distribution, wind speed, turbulence and surface characteristics of the object in a complicated way. Resuspension or evaporation as well as interactions with gaseous pollutants also occur after the particles have been deposited. It would therefore be expensive and complicated to try to estimate the particle deposition from size-segregated concentration measurements and meteorological parameters, because the parameters vary in time necessitating large numbers of short time measurements. The purpose with the surrogate surface is not to get exact deposition numbers representing the objects of interest, but to get standardised deposition fluxes that can be correlated with corrosion rates.

This paper presents the development of a passive sampler for particles and the results of the field programme. Results for nitric acid and dose–response functions obtained for all pollutant effects will be presented elsewhere. Since PM_{10} measurements are performed in most major cities in Europe today, another aim was to see if the mass of particles deposited on the passive sampler (surrogate surface) correlates with the PM_{10} concentrations that were measured at several of the sites selected. If a good correlation is achieved, the corrosion rate at sites with PM_{10} measurements but no surrogate surface could be estimated. In marked contrast to gaseous pollutants, particulate matter represents, of course, a mixture of different materials, which have different potential for both soiling and corrosion. Therefore, after determination of deposited mass, the surfaces were analysed for water-soluble ions. Dose–response functions for materials use annual average values for environmental and pollutant parameters.

Experimental

Tests of different surrogate surfaces

The development of the passive sampler was undertaken by the Swedish Environmental Research Institute (IVL) based on an earlier passive sampler for particle collection that consisted of a vertically-mounted diffusive sampler [3]. This sampler utilised a Teflon membrane as the target surface, with usually four samplers mounted perpendicular to each other. The current trial examined a number of alternative materials and sampler shapes. One immediate concern was that flat samplers, though replicating what happens on building surfaces, might not be ideal for field sampling where particulate matter might largely emanate from a single direction. Another shape of surface that receives particles from all directions was developed and tested in parallel. It consists of a vertically mounted 10-mm-diameter cylinder.

Five different materials were tested: glass, Teflon, polycarbonate, aluminium oxide and stainless steel. The glass and stainless steel were also tested with two different roughnesses of the surface by exposing plain glass and glass fibre filters and also stainless steel foil (0.05-mm thick) and stainless steel mesh (thread diameter 0.080 mm and an aperture of 0.125 mm). In all cases 25-mm discs were used. A plastic vial with a hollow lid was used for all materials in order to get comparable results. The materials presented as cylinders were glass, Teflon and stainless steel. A sketch of the samplers is shown in Fig. 1.

Three replicates of each type and material were tested at three sites: Patission (central Athens, 37°35′ N 23°26′ E), Montelibretti (in a rural area about 30 km north of Rome, 42° 06′ N 12°38′ E) and Middlesex University in London (51°36′ N 0°08′ W). The samplers were protected from rain by mounting them under a large roof. After one to two months exposure they were analysed in Sweden. The mass was determined by weighing the surfaces before and after exposure.

All surrogate surfaces were equilibrated for 24 h before weighing in the weighing room at a temperature of 20°C and 50% relative humidity (r.h.). It was not possible to accurately determine the weight of the deposited particles on the glass (flat and cylindrical) and the cylindrical stainless steel, as the samplers were too heavy to tare on the balance used. The surfaces were then leached in 4 mL de-ionised water and the Cl^-, NO_3^-, SO_4^{2-}, NH_4^+, Ca^{2+}, Mg^{2+}, Na^+ and K^+ concentrations in the leachate were analysed using ion chromatography.

Monitoring at the corrosion sites

The Teflon samplers selected (see discussion) were exposed at the network of test sites in the well established UNECE ICP Materials Programme (http://www.corr-institute.se/ICP-Materials), which consisted of 30 (27 European) test sites from 15 countries throughout Europe, see Fig. 2. Of these sites, 17 are urban e.g. Rome, Madrid, Berlin, Paris and London. A rectangular Teflon filter was wound around a 10-mm-diameter PVC tubing and held in place by a small clip (Fig. 3). The exposed area was 6.28 cm^2. This area was used to calculate the deposition. One set of surrogate surfaces was used for correlation with the corrosion rates for the specimens in an unsheltered position, partly protected from rain but not from wind, see Fig. 3. Rain or fog droplets falling with a slope smaller than about 12° from the horizontal hit the surrogate surface. If the size of these deposited droplets becomes large enough, they may run off the surface and remove material already deposited. Six samplers were exposed for 2 months to make up a one-year sampling period.

The surrogate surfaces used for correlation with the corrosion rates for materials in sheltered positions were mounted inside an aluminium box, which was open at the bottom, and thus were sheltered from rain and partly from wind. This passive sampler was exposed for one year. The Teflon filters were analysed for deposited particle mass and some water-soluble salts as described above. In addition, a number of urban sites were studied to look in more detail at some of the controls on deposition and soiling. The amount (mass) of deposited particles in wind-protected and wind-exposed positions were also compared to the particle (PM_{10}) concentration. PM_{10} measurements were obtained from a number of sites operated by local or regional networks (using different instrumentation at different sites; however, the methods should be equivalent to the EU reference method).

Results and discussion

Tests of surrogate surfaces

The results from analyses of the different surrogate surfaces at Patission station in Athens (26 February 2002 to 26 March 2002), Middlesex University near London (7 March 2002 to 2 May 2002) and Montelibretti outside Rome (29 March 2002 to 10 May 2002) are shown in Table 1. The average depositions and standard deviations are expressed in μg cm^{-2} $month^{-1}$. The water-soluble masses are calculated from the mass of analysed ions (i.e., no corrections for any crystallization water have been made).

From Table 2 it can be seen that the deposition to a rough surface is higher than to a smooth surface of the same material. Ammonium and potassium have been excluded because the depositions were so small that the figures are close to the detection limits. In order to see if the direction chosen for the flat surfaces was representative, the deposition has been compared to the average deposition in all directions (cylindrical shape). It is obvious that the direction chosen for the flat surfaces in Athens received very little deposition, which influenced the final decision to utilise a cylindrical sampler.

The ratios between different materials are presented in Table 3, from where it can be seen that glass, polycarbonate and aluminium oxide generally gave higher deposition of most ions than Teflon. This is likely to be due to reactions between the materials of the surrogate surfaces and acidic gases such as sulfur dioxide, nitric acid and hydrochloric

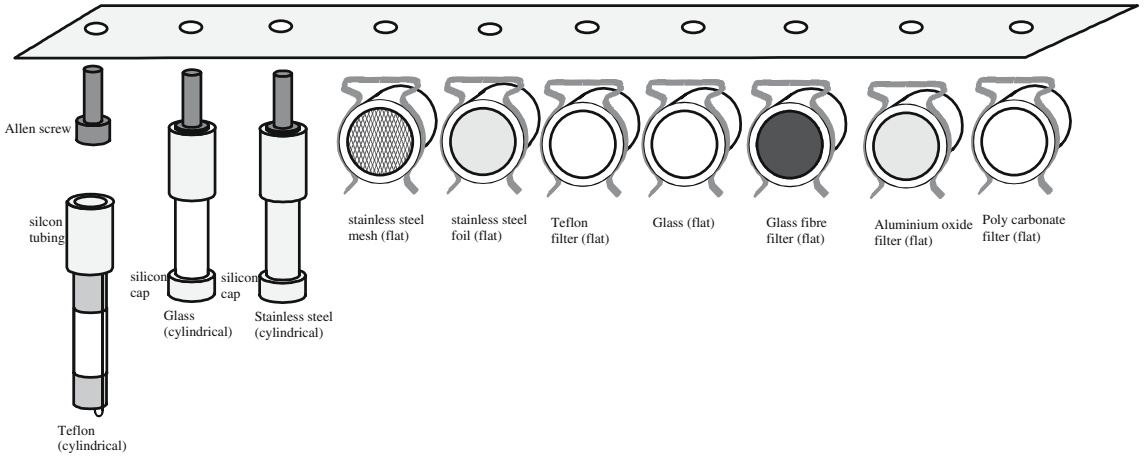

Fig. 1 Sketch of the tested surrogate surfaces

Fig. 2 Map showing the stations (*red circles*). Four pairs of co-located urban and rural sites are *encircled*

acid. To examine if electrostatic forces could increase the deposition on Teflon, this deposition was compared to that on stainless steel of similar shape. In most cases there are rather small differences. In Rome, however, the flat Teflon surface receives more sodium and chloride, and the cylindrical Teflon surface receives more calcium and sulfate than the corresponding stainless steel surfaces. This is difficult to explain and should perhaps be investigated further. In general, the sodium and chloride depositions correlate as well as the calcium and sulfate. The Teflon surface, however, does not seem to collect more than the stainless steel surface.

We considered that the cylindrical Teflon offered most advantages: it measures the deposition in all directions, which prevents any necessity to predict the prevailing direction of maximum deposition. The results were also similar to cylindrical steel (and glass, except for the release of sodium from glass). Importantly Teflon had the advantage that it could be pre-weighed and used to measure the total mass. The other two cylindrical samplers were too heavy for balances of sufficient accuracy for the predicted (and measured) particle masses. Soiling can also be measured on the Teflon filter via loss of light reflectance.

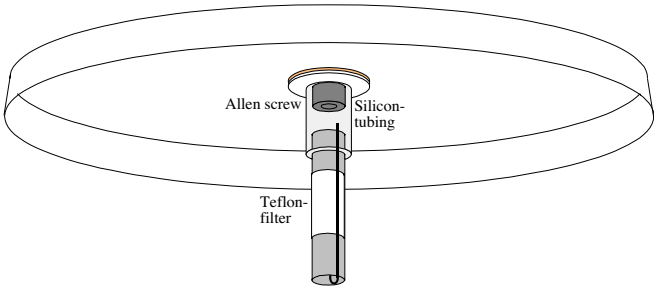

Fig. 3 Surrogate surface used in the broad field and targeted field programs

Particle deposition in unsheltered specimen position

The deposited mass varied between < 1 μg cm^{-2} $month^{-1}$ (detection limit) and 417 μg cm^{-2} $month^{-1}$ with an average of 32 μg cm^{-2} $month^{-1}$ on a bimonthly basis (every two months). The corresponding range for the annual basis (time weighted average from the bimonthly) was 4–138 μg cm^{-2} $month^{-1}$.

The average chemical composition is shown in Fig. 4. The weight of the analysed water-soluble ions correlated well with the total mass (y=0.30x−1.7, r^2=0.96) on an annual basis (see Fig. 5). On average 76% of the mass was not identified and was believed to mainly consist of water-insoluble material. The fraction of the unidentified mass did not vary much between the sites; the standard deviation was only ±7% on an annual basis. Since the filters were weighed at 50% r.h., this fraction may also contain water. Analysis of the water-insoluble fraction was not part of the project. The average ion balance is shown in Fig. 6. There is an excess of cations (29%), implying that anions are missing. Coarse particles have higher deposition velocities than fine particles and are normally alkaline and should therefore contain carbonate [4]. Equipment to analyse the carbonate content was not available here and the sample amount was too small for analysis of the alkalinity. Organic anions were not analysed either. Lee and Longhurst [5] studied the dry deposition to a bulk collector at an urban site and found higher calcium deposition than non-marine sulfate deposition. They also found a loss of acidity in the bulk collector compared to a wet-only collector. If all the

Table 1 Deposition (μg cm^{-2} $month^{-1}$) of total mass and some ions to different surrogate surfaces. Average and SD are given (n=3)

	Total mass	Cl^-	NO_3^-	SO_4^{2-}	NH_4^+	Ca^{2+}	Mg^{2+}	Na^+	K^+	Analysed mass
Athens										
Polycarbonate filter	18±8	0.2±0.2	0.9±0.8	2.0±0.3	0.3±0.1	0.7±0.6	0.0±0.0	0.4±0.2	0.0±0.0	4.6±2
Aluminium oxide filter	24±10	0.5±0.1	1.9±0.2	7.6±0.4	0.9±0.1	0.9±0.3	0.0±0.0	0.3±0.0	0.0±0.0	12.3±0.6
Teflon filter	10±1	0.4±0.1	0.5±0.0	0.5±0.0	0.0±0.0	0.6±0.1	0.0±0.0	0.3±0.0	0.0±0.0	2.4±0.2
Plain glass		0.7±0.4	2.2±0.1	1.6±0.2	0.0±0.0	2.0±0.9	0.1±0.0	1.8±0.1	0.2±0.1	8.6±0.9
Glass fibre filter	33±16	1.7±0.1	3.7±0.1	15±0.7	0.0±0.0	1.9±0.6	0.2±0.0	5.3±0.7	0.4±0.1	27.8±1.9
Stainless steel foil	23±22	0.4±0.4	0.7±0.8	0.9±0.6	−0.2±0.01	1.7±1.4	0.1±0.0	0.3±0.2	0.0±0.0	3.9±3.4
Stainless steel mesh	34±14	1.1±0.9	1.2±0.4	1.4±0.4	−0.1±0.0	2.3±0.8	0.1±0.0	0.6±0.5	0.2±0.3	6.7±3.3
Cylindrical Teflon	90±14	5.0±0.5	2.9±1.5	3.6±0.5	−0.2±0.2	3.2±0.6	0.4±0.1	3.9±0.5	0.2±0.0	19±4
Cylindrical glass		5.5±0.4	3.2±0.2	4.2±0.2	0.2±0.0	3.3±0.2	0.4±0.0	3.9±0.3	0.3±0.0	21±1
Cylindrical stainless steel		5.5±0.3	3.0±0.1	4.9±0.3	0.2±0.0	3.7±0.5	0.5±0.0	3.9±0.4	0.2±0.0	22±1
London										
Polycarbonate filter	22±13	3.2±2.6	1.4±0.4	1.9±1.1	0.0±0.0	0.7±0.5	0.3±0.2	2.6±1.7	0.1±0.1	10.1±6.5
Aluminium oxide filter	27±5	2.4±0.3	1.7±0.0	3.5±0.7	−0.1±0.0	1.6±0.3	0.3±0.0	1.7±0.2	0.0±0.0	11.1±0.9
Teflon filter	40±4	2.1±0.3	0.8±0.1	1.5±0.1	0.2±0.0	1.3±0.3	0.2±0.0	1.3±0.1	0.1±0.0	7.6±0.5
Plain glass		3.1±0.7	1.2±0.3	1.6±0.2	0.0±0.0	1.5±0.2	0.3±0.0	2.6±0.5	0.1±0.0	10.4±0.6
Glass fibre filter	18±12	3.7±0.4	2.1±0.0	6.5±0.5	0.0±0.0	0.9±0.2	0.2±0.0	5.1±0.8	0.4±0.0	18.9±1.9
Stainless steel foil	21±1	1.8±0.1	0.3±0.3	1.1±0.1	−0.1±0.0	0.9±0.1	0.2±0.0	1.2±0.2	0.0±0.0	5.3±0.6
Stainless steel mesh	42±8	3.1±1.7	1.0±0.2	2.7±0.8	−0.1±0.0	2.3±0.5	0.3±0.1	2.1±1.0	0.1±0.1	11.6±4.3
Cylindrical Teflon	60±16	5±2	2.3±0.4	4.1±1.4	0.0±0.0	2.5±0.8	0.4±0.1	3.4±1.0	0.0±0.0	18±4
Cylindrical glass		10±2	2.2±0.5	3.6±0.7	0.0±0.0	1.8±0.4	0.6±0.1	6.7±2.4	0.0±0.0	25±6
Cylindrical stainless steel		7±1	2.2±0.2	3.5±0.3	0.0±0.0	1.5±0.2	0.5±0.0	4.9±1.0	0.0±0.0	20±3
Rome										
Polycarbonate filter	31±10	0.4±0.3	1.3±0.3	0.9±0.7	0.1±0.1	0.9±0.6	0.1±0.0	0.5±0.0	0.2±0.2	4.4±2
Aluminium oxide filter	31±9	0.7±0.2	1.1±0.1	1.7±0.3	−0.2±0.0	1.9±0.4	0.1±0.1	0.3±0.2	0.0±0.0	5.6±1.1
Teflon filter	51±7	0.6±0.1	1.0±0.2	0.5±0.1	0.2±0.1	1.2±0.2	0.1±0.0	0.4±0.1	0.1±0.0	4.1±0.7
Plain glass		0.4±0.2	1.5±0.2	0.8±0.2	−0.1±0.0	2.8±0.7	0.3±0.1	1.6±0.2	0.1±0.0	7.4±1.3
Glass fibre filter	71±10	1.5±0.4	2.5±0.0	3.4±0.0	0.0±0.0	2.3±0.1	0.2±0.0	4.3±0.6	0.6±0.0	14.9±0.9
Stainless steel foil	15±4	0.1±0.0	−0.1±0.1	0.2±0.1	−0.1±0.0	1.0±0.1	0.1±0.0	0.1±0.0	−0.1±0.0	1.1±0.4
Stainless steel mesh	52±28	0.4±0.3	0.8±0.4	0.9±0.6	−0.1±0.1	3.7±1.9	0.2±0.1	0.2±0.2	0.0±0.1	6.3±3.7
Cylindrical Teflon	51±15	0.6±0.2	1.9±0.1	0.8±0.2	0.1±0.2	2.2±0.4	0.1±0.0	0.5±0.2	0.0±0.0	6.4±1.1
Cylindrical glass		0.3±0.2	1.6±0.6	0.4±0.1	0.1±0.0	0.7±0.1	0.1±0.0	0.4±0.1	0.0±0.0	3.7±1.1
Cylindrical stainless steel		0.4±0.2	1.4±0.6	0.4±0.1	0.0±0.0	0.6±0.2	0.1±0.0	0.3±0.2	0.1±0.0	3.2±1.3

missing anions here consist of carbonate, this would be another 7% of the average mass.

Bardouki et al. [6] found that the anion deficiency correlated well with the calcium concentration in air. This was also observed for the deposition here (anion deficien-

Table 2 Ratios between depositions to surfaces of different structure or orientation

	Total mass	Cl^-	NO_3^-	SO_4^{2-}	Ca^{2+}	Mg^{2+}	Na^+	Analysed mass
Glass fibre filter/plain glass								
Athens		2.2	1.7	9.4	0.9	1.1	3.0	3.2
London		1.2	1.7	4.1	0.6	0.8	1.9	1.8
Rome		3.8	1.7	4.2	0.8	0.6	2.7	2.0
Stainless steel mesh/stainless steel foil								
Athens	2.7	3.0	0.8	0.2	1.7	2.3	0.7	0.7
London	2.0	1.8	4.0	2.5	2.5	2.0	1.7	2.2
Rome	3.4	6.5	−8.6	4.2	3.8	4.1	3.2	5.6
Plain Teflon/cylindrical Teflon								
Athens	0.1	0.1	0.2	0.1	0.2	0.1	0.1	0.1
London	0.7	0.4	0.4	0.4	0.5	0.5	0.4	0.4
Rome	1.0	1.0	0.5	0.5	0.5	0.9	0.8	0.6

Table 3 Ratios between depositions to different materials of similar shape

	Total mass	Cl^-	NO_3^-	SO_4^{2-}	Ca^{2+}	Mg^{2+}	Na^+	Analysed mass
Cylindrical stainless steel/cylindrical Teflon								
Athens		1.1	1.0	1.4	1.1	1.2	1.0	1.1
London		1.4	0.9	0.9	0.6	1.4	1.4	1.1
Rome		0.6	0.7	0.4	0.3	0.5	0.7	0.5
Stainless steel foil/plain Teflon								
Athens	2.2	0.9	1.3	2.1	3.1	1.8	0.8	1.6
London	0.5	0.8	0.3	0.7	0.7	0.8	0.9	0.7
Rome	0.3	0.1	−0.1	0.5	0.8	0.5	0.2	0.3
Plain glass/plain Teflon								
Athens		1.7	4.3	3.4	3.6	4.9	5.0	3.6
London		1.5	1.5	1.1	1.2	1.4	2.0	1.4
Rome		0.7	1.5	1.8	2.4	2.7	3.9	1.8
Polycarbonate/Teflon								
Athens	1.7	0.5	1.7	4.3	1.2	1.5	1.2	1.9
London	0.5	1.5	1.7	1.3	0.5	1.5	2.0	1.3
Rome	0.6	0.7	1.3	2.0	0.8	1.0	1.3	1.1
Aluminium oxide/Teflon								
Athens	2.6	5.4	3.4	7.5	2.9	8.9	5.0	4.6
London	0.7	1.1	2.1	2.3	1.3	1.3	1.3	1.5
Rome	0.6	1.2	1.1	3.7	1.6	1.1	0.7	1.4

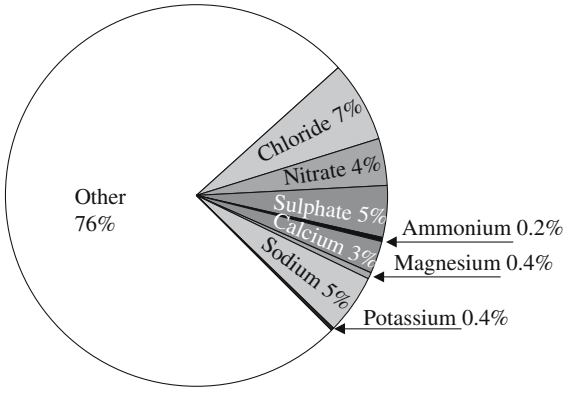

Fig. 4 Average chemical composition (percentage mass) of the particles deposited on the surrogate surface in the broad field experiment

cy=1.14×calcium deposition−4.4 nmol cm^{-2} $month^{-1}$, r^2=0.82 for the wind-exposed position).

Calcium was poorly correlated with Na^+ (r^2=0.54) and had an average Ca^{2+}/Na^+ ratio of 0.32, which should be compared to 0.022 for seawater. There must be other sources for Ca^{2+} than sea spray. The estimate of calcium emissions in Europe is very uncertain [7]. The main source is assumed to come from soils. The main industrial source is power production from smaller plants. The deposition of calcium was higher in urban areas than in background, which may reflect deposition of both soil and other re-suspended particles including from building materials.

In Fig. 7 it is evident that the non-marine sulfate deposition correlated well with the non-marine Ca^{2+} deposition (y=0.47x+1.6, r^2=0.94). The marine fractions were

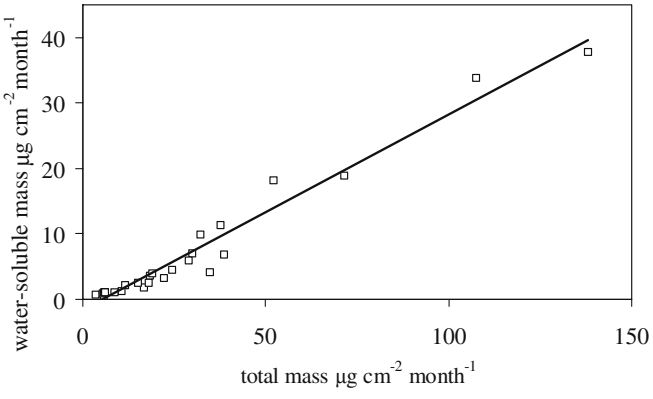

Fig. 5 Mass of deposited analysed water-soluble mass as a function of the deposited total mass in the broad field experiment, wind-exposed position

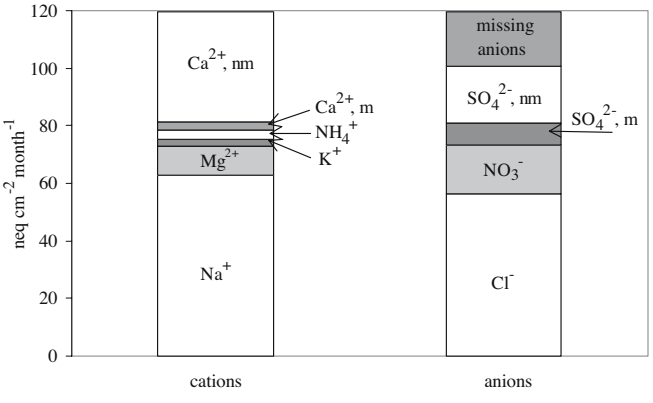

Fig. 6 Average ion balance between analysed cations and anions in the wind-exposed position

estimated from the Na^+ deposition. A reaction between SO_2 and a calcium salt (e.g. $CaCO_3$ or $CaCl_2$) could cause the good correlation between non-marine sulfate and calcium. Mineral aerosol particles react with SO_2 as well as HNO_3 in the air to form particles covered with sulfate and nitrate [8]. The correlation between deposited calcium and nitrate was, however, very poor here (r^2=0.66). The reactions can take place in the atmosphere as well as after the particles have deposited on the surrogate surface. Calcium sulfate can also be formed on a filter by reaction of deposited ammonium sulfate particles with calcium carbonate particles [9]. The relationship between sulfate and calcium in net-throughfall has earlier been studied using another shape of surrogate surface [10]. Deposited SO_2 reacted with calcium in intercellular spaces of spruce needles. The lifetime of calcium and sodium particles in the atmosphere is short (hours to days). The exposure time here was two months for the rain-protected surface and one year for the open-bottomed box. The mass transfer between the particles and the surrounding gases is in any event probably higher after deposition because they are not moving with the same speed as the wind. For these two reasons it seems likely that more gas molecules have reacted with the particles after they have been deposited compared to when they were dispersed in the atmosphere. Since both HNO_3 and SO_2 were measured alongside the particle deposition, deposition velocities (deposition flux/ambient concentration) could be calculated. The average deposition velocity for HNO_3 was 5.2±2.5 mm s^{-1} and 1.2±1.1 mm s^{-1} for SO_2. The deposition velocities must be zero at the start of exposure and increase with the particle deposition. When the deposition velocity for HNO_3 for the different sites was plotted as a function of the sodium deposition to the wind-exposed surrogate surface, a clear positive correlation was found. This was also the case when the deposition velocity for SO_2 was plotted as a function of the anion deficiency in the analysed ions. The same plots were repeated for the sheltered position. The deposition velocities were 1.7±1.5 mm s^{-1} and 0.4±0.6 mm s^{-1} for HNO_3 and SO_2, respectively. These deposition velocities also correlated well with the sodium and anion deficiencies, respectively.

When the annual averages for all stations were plotted, the SO_4^{2-}/Ca^{2+} slope of the regression line was not unity as in gypsum, but 0.47. The Ca^{2+} and non-marine SO_4^{2-}

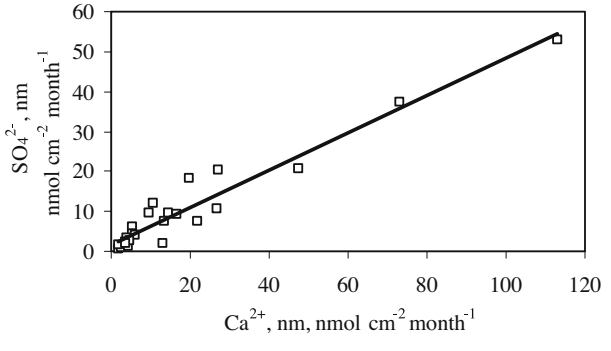

Fig. 7 Non-marine sulfate deposition as a function of non-marine calcium deposition

depositions were highest at the sites in Lisbon, Athens, London, Berlin, Krakow and Moscow. It should be noted that individual sites cannot be representative of an entire city or region and interpretation in this section refers to the specific locations sampled. The two ions correlated fairly well on a bimonthly basis too (r^2=0.76). The marine fraction of the calcium deposition was very small (< 7%).

In some cases, a rural station was located not too far from the urban site. Four such urban–rural pairs are encircled on the map in Fig. 2. The non-marine sulfate deposition was higher at the urban sites than at the rural, especially in the winter and sometimes in the spring (Fig. 8). Since the anion deficiency and the non-marine sulfate deposition were both correlated with calcium deposition, and the fact that the sum of missing anions and non-marine sulfate deposition was similar to the non-marine calcium deposition, it was hypothesised that sulfate mainly originates from a reaction between calcium and sulfur dioxide. The anion deficiency plus the non-marine sulfate deposition correlated to the calcium deposition according to the expression 1.02×calcium deposition−0.3 neq cm^{-2} $month^{-1}$, r^2=0.95.

The chloride deposition correlated very well with the sodium deposition (y=0.88x+1.0, r^2=0.99) for annual averages, see Fig. 9, but the average Cl^-/Na^+ ratio was only 0.90 on a molar basis. The Cl^-/Na^+ ratio had a minimum in summer and a maximum in winter. This situation has also been observed by Bardouki et al. [6]. In seawater the Cl^-/Na^+ ratio is 1.17. The loss of chloride ions is probably caused by reaction between NaCl and HNO_3 or other acidic gases to form HCl [11]. The average nitrate deposition equals the missing chloride deposition within 1%, suggesting that the nitrates consist of $NaNO_3$. The sum of NO_3^- and Cl^- depositions were therefore plotted as a function of the sodium deposition to see if the reaction HNO_3+NaCl→$NaNO_3$+HCl could explain the nitrate deposition flux. The regression line was 1.05×Na deposition +10.7 nmol cm^{-2} $month^{-1}$, r^2=0.98. It was therefore concluded that most of the nitrates was $NaNO_3$.

According to Fig. 10 the Mg^{2+} deposition also correlated well with Na^+ deposition when the results from Berlin were removed (y=0.09x+1.0, r^2=0.97). The slope was 0.09, which should be compared to 0.11 for seawater. The Mg^{2+}/Na^+ ratio was even closer to that for seawater at the sites with the highest Na^+ deposition (Lisbon, Venice, London and Casaccia). Berlin had the highest NaCl deposition but with a very small Mg^{2+} deposition. It should be noted that this site is very close to a highway and so the origin of this salt was likely to be from the road, which is also suggested by the clear winter maximum observed (Figs. 8 and 11). The deposition results from Berlin were therefore excluded from the correlations with non-marine fractions.

The Na^+ deposition was generally highest in winter (Fig. 11). This is also likely to be due to the use of salt on roads for de-icing purposes.

The dry deposition of ammonium is very low here compared to calcium deposition. Van Borm et al. [12] measured the volume mean diameter for different elements in Antwerp. It was larger for $CaSO_4$ (5.5 μm) than for NaCl

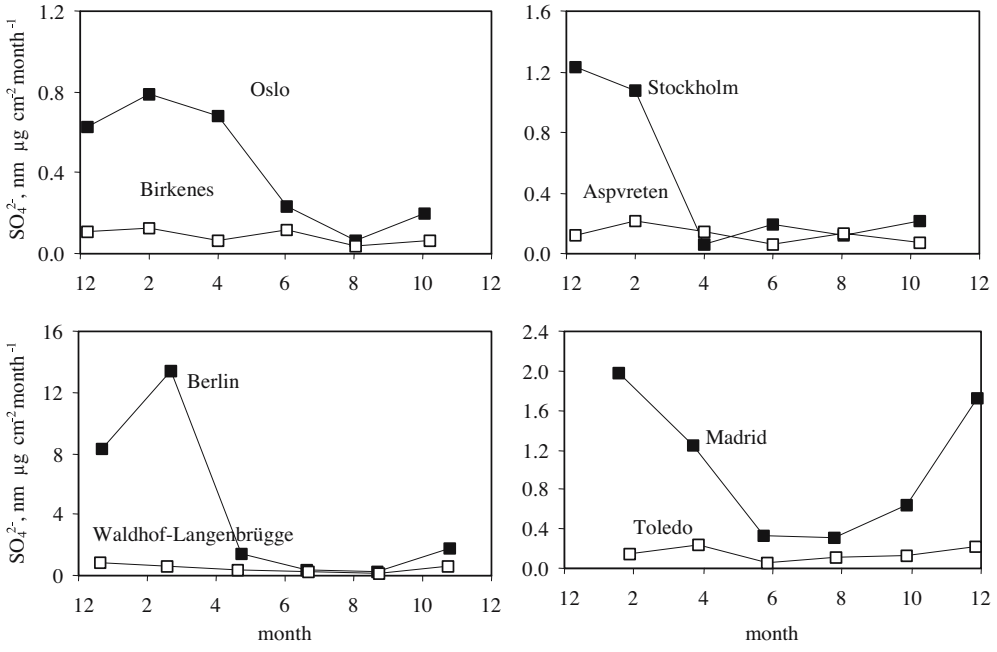

Fig. 8 Non-marine sulfate deposition as a function of the middle of the exposure interval at four urban sites (*filled squares*) and their closest background site (*open squares*)

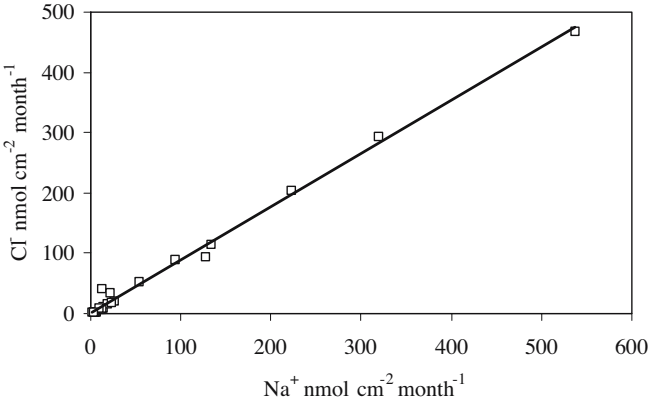

Fig. 9 Chloride deposition as a function of sodium deposition

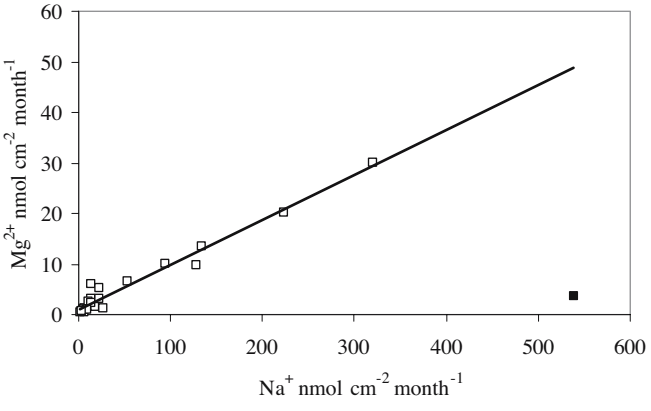

Fig. 10 Magnesium deposition as a function of sodium deposition. The Berlin measurement (*filled square*) has been excluded from the regression line

(2.7 µm) and for $(NH_4)_2SO_4$ (0.6 µm). Bardouki et al. [6] also found an increasing particle size in the order $NH_4^+ < Na^+ < Ca^{2+}$. The reason for the low ammonium deposition is probably that mainly large particles are deposited on the surrogate surface [13] and that these particles contain a very small amount of ammonium [6, 14, 15]. The fine ammonium sulfate particles that have been deposited can also lose their ammonium by reaction with carbonate followed by ammonia volatilisation [9].

The light reflectance of the filters was measured to estimate the soiling of objects. For fine particles the loss of reflectance (expressed as the logarithm of the ratio between the reflectance before and after exposure) is a fairly good measure of the elemental carbon (graphite) amount per unit exposed area. Since graphite is the main light-absorbing substance in ambient air [16] it was used here to test if it correlated with the other chemical species. The correlation was not strong for any of the analysed species. The best correlation was found with the non-marine sulfate deposition (y=0.012x +0.013, r^2=0.66, see Fig. 12). This may reflect the dominance of traffic emissions, especially in cities. Road traffic sources are known to be the main factor influencing annual mean levels of SO_2 in London (e.g. see ref. [17]) as well as dominating emissions of particulate matter. In other locations, continued use of coal may also contribute to emissions of both pollutants.

The response as a function of graphite deposition depends on the size of the graphite particles [18]. A response factor of 10 m^2 g^{-1} is often used [19]. By dividing the R_0/R per unit time by this constant an average elemental carbon deposition of 0.3 µg cm^{-2} month^{-1} is obtained. The elemental carbon mass fraction of the average mass is thus of the order of 1% (cf. Fig. 4).

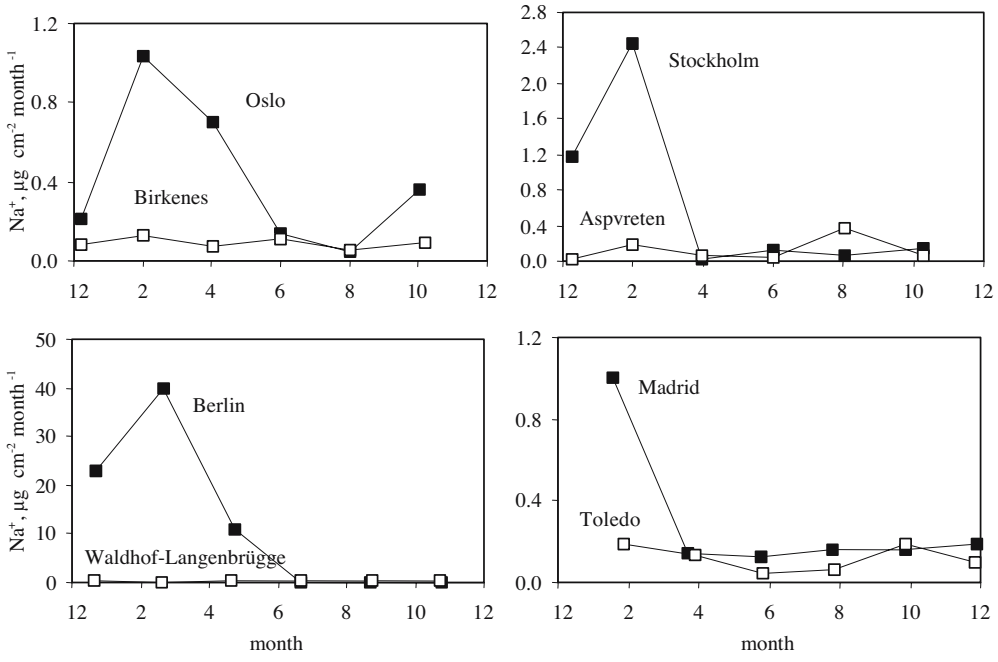

Fig. 11 Sodium deposition as a function of the middle of the exposure interval at four urban sites (*filled squares*) and their closest background site (*open squares*)

Particle deposition in sheltered position

The average total mass of deposited particles inside the box was only 26% of the average mass in the wind-exposed position. The average fractions of the unidentified material were, however, very similar (77% compared to 76% in the wind-exposed position). The fraction of analysed water-soluble mass in the wind-protected position correlated surprisingly well to the same fraction in the wind-exposed position (y=0.25x−0.053, r^2=0.84), see Fig. 13. Even though the fractions of analysed water-soluble masses were similar in the wind-protected and wind-exposed positions, the relative abundance of different ions varied. There was more calcium, a higher anion deficiency and less sodium chloride and magnesium in the wind-protected position compared to the wind-exposed position, see Fig. 14. The ion balance for the wind-protected position gives a 24% excess of cations. The anion deficiency for the samplers in the box was −0.73×calcium deposition+0.6 nmol cm^{-2} month^{-1}, r^2=0.96 if the result from Berlin, which had an extremely high NaCl deposition, was excluded. The sum of missing anions and non-marine sulfate deposition also correlated well to the calcium deposition here with a regression line of 1.01×calcium deposition−0.7 neq cm^{-2} month^{-1}, r^2=0.93.

The reaction of HNO_3 with the deposited sodium chloride particles seems to be a little more pronounced here compared to the wind-exposed position. The average Cl^-/Na^+ ratio was only 0.67 on a molar basis compared to 0.90 for the wind-exposed position. There was also relatively more nitrate compared to sodium in the wind-protected position. A higher nitrate and non-marine sulfate deposition, which is caused by reactions with acidic gases, might be explained by the longer exposure time of these samples compared to the wind-exposed. They were exposed for one year and the samples in the wind-exposed position for two months. The missing

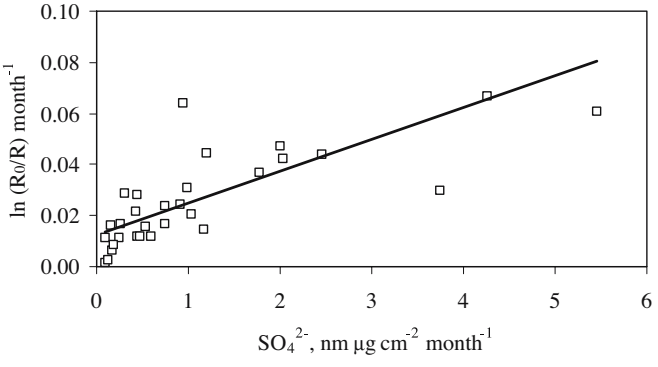

Fig. 12 Natural logarithm of the ratio between light reflectance of the filter before and after exposure divided by exposure time as a function of the non-marine sulfate deposition

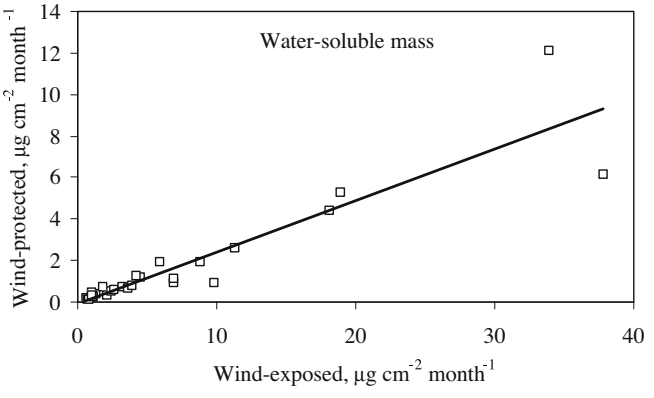

Fig. 13 Mass of analysed water-soluble ions deposited on the surrogate surface mounted in the main box (sheltered from rain and partly from wind) as a function of the same mass deposited on the surrogate surface mounted under a small metal lid (sheltered from rain coming from above, but not from wind)

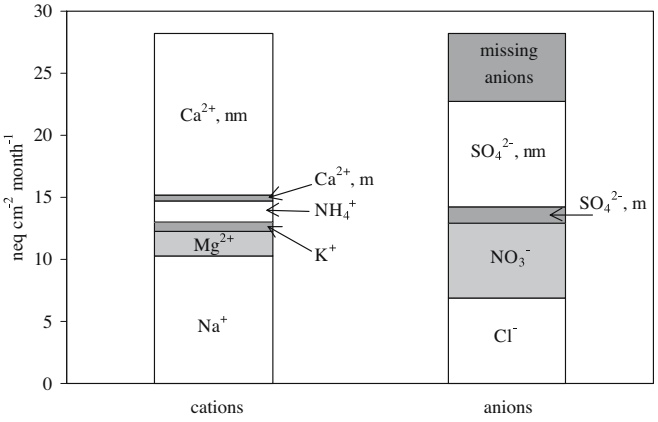

Fig. 14 Average ion balance between analysed cations and anions in the wind-protected position

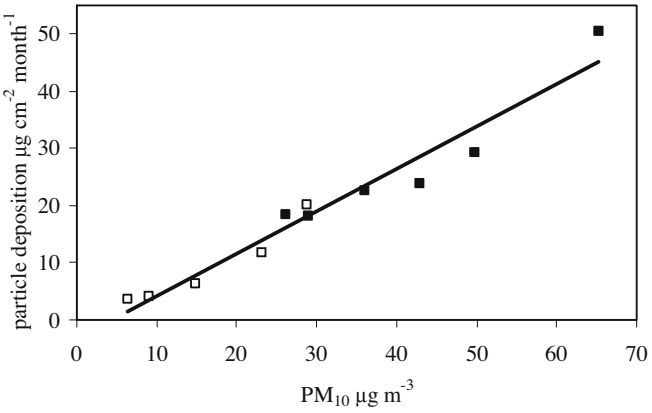

Fig. 15 Particle deposition to the surrogate surface in the wind-exposed position at background (*open squares*) and urban stations (*filled squares*) as a function of PM_{10} concentration

chloride almost corresponded to the nitrate deposition here and the regression equation for the sum of nitrate + chloride depositions was 1.10×Na deposition+3 nmol cm^{-2} $month^{-1}$, r^2=0.98. Eleftheriadis et al. [20] found that particulate sulfate and nitrate were strongly correlated with one or more particulate base cations in Athens. More recently Varotsos et al. [21] analysed the PM_{10} measurements in Athens and found persisting long-range power-law correlations from about 4 h to 9 months.

Comparison of deposition flux with PM_{10} concentrations

Particles are deposited on the surrogate surface by diffusion and impaction. For coarse particles that are mainly deposited by impaction, the efficiency increases with aerodynamic particle diameter. PM_{10} sampling is set up to mimic the fraction of particles that penetrate beyond the larynx. The sampling efficiency as a function of diameter therefore decreases with the aerodynamic diameter of the particle. According to the definition [22], it is 100% for 1-μm particles, 55.1% for 10-μm particles and 4.1% for 15-μm particles. One should therefore not expect a high correlation between passively collected particles and PM_{10}. As mentioned earlier, the PM_{10} values were obtained from other projects. Different equipment was used at different sites and the samplers were not always co-located with the passive particle collector. The correlation was, however, fairly good (r^2=0.60) even for individual bimonthly sampling periods. When annual means were compared, the correlation was surprisingly good (y=0.74−3.2, r^2=0.95, Fig. 15). The urban and background sites all showed the same correlation with the PM_{10} concentrations, see Fig. 15. The slope corresponds to a deposition velocity of 2.3±0.4 mm s^{-1}.

Three stations had to be removed to get this high correlation. The stations in Berlin, Athens and Krakow are all situated very close to roads with intensive traffic. The deposition velocities for these sites were 18, 7.1 and 4.3 mm s^{-1}, respectively. No chemical speciation of the PM_{10} samples was available, only the mass. A comparison to see if a similar mixture of particles was collected actively and passively could therefore not be made. The good correlation could possibly have been caused by similar size distributions and wind speeds at the eleven sites. It seems here as though the deposited mass to the cylindrical surface can be estimated from the PM_{10} concentration at all places that are far from sources. More investigations are, however, needed in order to generalise this correlation.

The deposition velocity depends on the shape and orientation of the surface. This particular surface receives particles all the time, independent of wind direction. Many surfaces, however, are facing one direction from which they receive most of their particle deposition. If the particle deposition is divided by the projected area of the surrogate surface the flux will more closely resemble the particle deposition to a flat surface facing the wind. The projected area equals the total area divided by π. The deposition to a flat area should therefore be a factor of π higher than the fluxes presented here. On the other hand a flat surface does not receive particles when the wind is coming from the opposite direction to the one the surface is facing. The flux obtained from the surrogate surface using the projected area will thus be higher than the actual deposition to a flat surface in a fixed position if the wind comes from different directions during the exposure time. It was therefore considered better to use the totally exposed area of the surrogate surface for the flux calculation. One surrogate surface can of course not represent all the surfaces at risk from atmospheric corrosion. This surrogate surface will be used as a "standardised" cost-efficient passive particle collector in several projects in which corrosion rate is compared to particle deposition and other environmental factors.

Nicholson [23] has reviewed experimental dry deposition measurements. Surrogate surfaces have often been used, but they are normally positioned horizontally, not vertically as here. Pesava et al. [24] measured the deposition of artificial fine particles (0.6- to 0.8-μm mean diameter) to a 3-cm cube. The deposition velocity to the vertical side facing the wind was about 0.7 mm s^{-1} for a roughness of 0.08 mm and 1.4 mm s^{-1} for a roughness height of 0.2 mm. The deposition velocities for these fine particles (roughness height 0.2 mm)

to the horizontal sides were very similar to the vertical one facing the wind. It was 0.9 mm s^{-1} for upward and 0.7 mm s^{-1} for the downward facing side. It is not surprising that a higher deposition velocity was obtained in this project because the deposition velocity increases with aerodynamic diameter of the particles and large particles from road abrasion and erosion occur in ground-level air. Vawda et al. [25] measured the dry deposition velocity of different ions in ambient particles to a horizontal Teflon tile at a rural site. The deposition velocities for ammonium, nitrate and sulfate were about 1, 2 and 2 mm s^{-1}, respectively.

A similar plot for the passive particles in the aluminium box (wind-protected position) with the PM_{10} concentration was not as good (r^2=0.64). The average deposition velocity was 0.6±0.4 mm s^{-1}. There could be several reasons for this. The samplers were exposed for six times longer period than the wind-exposed sampler. This increases the risk for contamination, and insects sometimes lived in the boxes. The wind velocity of the air surrounding the surrogate surface could be a complicated function of the wind speed outside the box. The function could be affected by where the box was mounted. This was the first project in which a surrogate surface for particulate matter was exposed inside a box and it was beyond the aim of this project to investigate the mechanisms behind the particle deposition. This could, however, be a subject for future studies.

Conclusions

A simple passive particle collector for estimating the dry deposition to objects of cultural heritage has been developed. Monitoring results during one year have shown that the deposited Na^+, Ca^{2+}, Cl^-, SO_4^{2-} and NO_3^- ions constitute 24% of the deposited particle mass on average. The concentrations of these are higher in urban areas than in rural positions. From the theory for particle deposition we can conclude that the mass of deposited particles mainly belong to the coarse mode. The deposited nitrates originate from gaseous nitric acid that has reacted with deposited sodium chloride, mainly of marine origin. Deposited calcium correlates well with the anion deficiency that we observe and with deposited anthropogenic sulfate. It seems very likely that the deposited sulfates originate from a reaction between sulfur dioxide and basic calcium compounds.

The deposition to a partly wind sheltered sampler is fairly proportional to a wind-exposed one. The deposited mass correlated surprisingly well to the PM_{10} concentration with an average deposition velocity of 2.3 mm s^{-1}.

Acknowledgements Funding has been received from the Foundation of the IVL Swedish Environmental Research Institute and MULTI-ASSESS, a research project supported by the European Commission under the Fifth Framework Programme Key Action City of Tomorrow and Cultural Heritage. We want to acknowledge all the participants in the MULTI-ASSESS project and all the people that have been involved in the sampling.

References

1. Svensson J-E, Johansson L-G (1993) J Electrochem Soc 140:2210–2216
2. Strandberg H (1998) Atmos Environ 32:3511–3520
3. Ferm M (2004) Use of passive samplers in connection with atmospheric corrosion studies (International Workshop on Atmospheric Corrosion and Weathering Steels, Colombia 27 Sept 1 Oct 2004)
4. Mészáros E, Barcza T, Gelencsér A, Hlavay J, Kiss G, Krivácsy Z, Molnár A, Polyák K (1997) J Aerosol Sci 28:1163–1175
5. Lee DS, Longhurst JWS (1992) Water Air Soil Pollut 64:635–648
6. Bardouki H, Liakakou H, Economou C, Sciare J, Smolík J, Ždmal V, Eleftheriadis K, Lazaridis M, Dye C, Mihalopoulos N (2003) Atmos Environ 37:195–208
7. Lee DS, Kingdon RD, Pacyna JM, Bouwman AF, Tegen I (1999) Atmos Environ 33:2241–2256
8. Dentener FJ, Carmichael GR Zhang Y, Lelieveld J, Crutzen PJ (1996) J Geophys Res 101:22869–22889
9. Mori I, Nishikawa M, Iwasaka Y (1998) Science Total Environ 224:87–91
10. Ferm M, Hultberg H (2004) Water Air Soil Pollut Focus 4:237–245
11. ten Brink HM, Spoelstra H (1996) J Aerosol Sci 27(Suppl 1): S667–S668
12. Van Borm WA, Adams FC, Maenhaut W (1989) Atmos Environ 23:1139–1151
13. Noll KE, Fang YP, Watkins LA (1988) Atmos Environ 22:1461–1468
14. Willison MJ, Clarke AG, Zeki EM (1985) Atmos Environ 19:1081–1089
15. Jacobson MZ (1999) Atmos Environ 33:3635–3649
16. Horvath H (1993) Atmos Environ 27A:293–317
17. Environmental Research Group (ERG) (2003) Air quality in London 2002. Tenth report of the London Air Quality Network ERG
18. Horvath H (1995) Atmos Environ 29:875–883
19. Huffman HD (1996) Atmos Environ 30:73–83
20. Eleftheriadis K, Balis D, Ziomas IC, Colbeck I, Manalis N (1998) Atmos Environ 32:2183–2191
21. Varotsos C, Ondov J, Efstathiou M (2005) Atmos Environ 39:4041–4047
22. CEN (1998) Air quality - determination of the PM_{10} fraction of suspended particulate matter - reference method and field test procedure to demonstrate reference equivalence of measurement methods. European Committee for Standardization EN 12341
23. Nicholson KW (1988) Atmos Environ 22:2653–2656
24. Pesava P, Aksu R, Toprak S, Horvath H, Seidl S (1999) Sci Total Environ 235:25–35
25. Vawda Y, Harrison RM, Nicholson KW, Colbeck I (1990) J Aerosol Sci 21:S201–S204